symmetry

MDPI

Article

Impact of Bioconvection and Chemical Reaction on MHD Nanofluid Flow Due to Exponential Stretching Sheet

Muhammad Imran Asjad [1], Noman Sarwar [1], Bagh Ali [2], Sajjad Hussain [3], Thanin Sitthiwirattham [4,*] and Jiraporn Reunsumrit [5]

1 Department of Mathematics, University of Management and Technology, Lahore 54770, Pakistan; imran.asjad@umt.edu.pk (M.I.A.); f2019109034@umt.edu.pk (N.S.)
2 Department of Applied Mathematics, Northwestern Polytechnical University, Xi'an 710072, China; baghalisewag@mail.nwpu.edu.cn
3 School of Aerospace and Mechanical Engineering, Nanyang Technological University, Singapore 639798, Singapore; sajjadgut@gmail.com
4 Mathematics Department, Faculty of Science and Technology, Suan Dusit University, Bangkok 10300, Thailand
5 Department of Mathematics, Faculty of Applied Science, King Mongkut's University of Technology North Bangkok, Bangkok 10800, Thailand; jiraporn.r@sci.kmutnb.ac.th
* Correspondence: thanin_sit@dusit.ac.th

Abstract: Thermal management is a crucial task in the present era of miniatures and other gadgets of compact heat density. This communication presents the momentum and thermal transportation of nanofluid flow over a sheet that stretches exponentially. The fluid moves through a porous matrix in the presence of a magnetic field that is perpendicular to the flow direction. To achieve the main objective of efficient thermal transportation with increased thermal conductivity, the possible settling of nano entities is avoided with the bioconvection of microorganisms. Furthermore, thermal radiation, heat source dissipation, and activation energy are also considered. The formulation in the form of a partial differential equation is transmuted into an ordinary differential form with the implementation of appropriate similarity variables. Numerical treatment involving Runge–Kutta along with the shooting technique method was chosen to resolve the boundary values problem. To elucidate the physical insights of the problem, computational code was run for suitable ranges of the involved parameters. The fluid temperature directly rose with the buoyancy ratio parameter, Rayleigh number, Brownian motion parameter, and thermophoresis parameter. Thus, thermal transportation enhances with the inclusion of nano entities and the bioconvection of microorganisms. The findings are useful for heat exchangers working in various technological processors. The validation of the obtained results is also assured through comparison with the existing result. The satisfactory concurrence was also observed while comparing the present symmetrical results with the existing literature.

Keywords: magnetohydrodynamics; chemical reaction; nanofluids; stretching sheet; bioconvection

Citation: Asjad, M.I.; Sarwar, N.; Ali, B.; Hussain, S.; Sitthiwirattham, T.; Reunsumrit, J. Impact of Bioconvection and Chemical Reaction on MHD Nanofluid Flow Due to Exponential Stretching Sheet. *Symmetry* **2021**, *13*, 2334. https://doi.org/10.3390/sym13122334

Academic Editor: Mina Teicher

Received: 11 October 2021
Accepted: 18 November 2021
Published: 5 December 2021

1. Introduction

The incompressible flow of viscous magnetic fluids across a boundary sheet is important in numerous industrial manufacturing processes. They can also be used in foamed and foam solids, porous rocks, microemulsions, and polymer blends, etc. Magnetohydrodynamics has a lot of applications in space sciences, generators, various machines, and drugs [1,2]. Abdal et al. [3] described how magnetohydrodynamics mixed the convection time-dependent stream of micro-polar nanofluids past a stretching/shrinking surface with radiations in the presence of a thermal source, multiple slips, and thermodiffusion. The influence of the slip on the time-dependent MHD mixing the convection of nanofluid through an extending sheet with a heat energy and electrical field was introduced by Daniel et al. [4]. Kumar et al. [5] discussed the influence of thermal radiation on MHD natural convection for nanofluids' heat transport on a vertical plate. Rashed [6] analyzed

the generation of entropy caused by radiation and the MHD impacts of varying thickness along a permeable spherical pipe. Poply et al. [7] deliberated a stretchable cylinder, with the stability assessment of a magnetohydrodynamics exterior velocity flow. Dawar et al. [8] studied the heat and mass transfer of micropolar liquid with a microstructural slip and chemical reaction over a stretchable sheet. Khan et al. [9] introduced the fixed element system of several slip impacts on an MHD time-dependent viscoelastic nanofluid stream through a porous extending sheet. Jabeen et al. [10] debated whether magnetohydrodynamic fluids in porous medium could linearly extend the sheet with a chemical reaction, heat absorption/generation, thermophoresis, and radiation.

The thermal conductivity of base fluids is improved by mixing nanoparticles. The base fluid can be lubricants, ethylene glycol, water and kerosene oil, etc. Processing industries, cancer therapy, cooling, biomedical and some engineering applications were among the first to use nanofluids. Choi et al. [11] were the first to show that nanofluids contained nanoparticles in 1995. Gopal et al. [12] discussed the impact of viscous dissipation in a numerical study of higher-order chemical reactions in electrically magnetohydrodynamic nanofluids. Ghasemi et al. [13] presented the impact of solar radiation on MHD that influenced the two-dimensional stagnation point flow and heat transfer of a nanofluid over a stretching surface. Krishna et al. [14] analyzed the absorption of radiation by a vertically moving permeable plate in the MHD convection flow of nanofluid. Hybrid nanofluids flowing through a nonlinear stretched cylinder with an inclined magnetic field were introduced by Abbas et al. [15]. Zainal et al. [16] examined the flow stability of an MHD hybrid nanofluid with a nonlinear shrinking/stretching sheet. Sreedevi et al. [17] illustrated the impact of slip effects and chemical reaction on heat and mass transportations in an unsteady hybrid nanofluid flow overextending surface using thermal radiation. Shoaib et al. [18] worked over a stretching layer and numerically investigated the rotating flow of the heat and mass transfer in a 3D MHD hybrid nanofluid with thermal radiation. Narender et al. [19] investigated the relation of viscid dissipation because of a convective stretchable surface with chemical reaction and thermal radiation. Rashid et al. [20] analyzed the flow of magnetohydrodynamic nanofluids and their thermal transfer past a stretching sheet through the impact of the nanoparticles' form.

The flow over a stretchable sheet has favorable applications in various fields of engineering. In the manufacturing of plastic sheet and wire drawing, some significant applications of flow through a stretched sheet of paper and glass production. Crane [21] was the first to define the steady flow through a stretching surface. Numerous authors have extended Crane's work by examining many physical processes, magnetic fields, the impacts of suction or injection, and heat transfer on such flow overextending sheets. Gupta et al. [22] studied the stretching flow with suction or injection. Yasmin et al. [23] addressed the study of thermal and mass transportation in the magnetohydrodynamic flow of micropolar fluid through a curved stretching surface. Swain et al. [24] established the impact of embedding in a permeable approach on MHD flow, thermal transport joule heating and viscous dissipation over a stretching surface. Reddy et al. [25] analyzed the influence of heat absorption/generation on the flux of magnetohydrodynamic copper and water nanofluid through a shrinking/stretching surface. Singh et al. [26] discussed the nonlinear magnetohydrodynamic flow of mass transpiration because of the permeable stretching sheet. Murtaza et al. [27] explained the heat transport and MHD flow on the bent extending sheet given nonlinear thermal conductivity. A numerical explanation of the magnetohydrodynamics of 2-D stagnation point flow to an extending sheet was presented by Narsingani et al. [28]. Ali et al. [29] deliberated passing an axisymmetric nanofluid stream through a stretched sheet with heat diffusion that has a time-dependent thickness influence on varying MHD. Ullah et al. [30] analyzed the suction/injection influence at the boundary of a magnetohydrodynamic curve hyperbolic fluid stream with an extended surface.

In 1961, Plat [31] proposed the idea of bio-convection. Biological polymer manufacturing, biotechnology and bio-sensors, as well as the testing and laboratory sectors, etc., are all examples of bioconvection applications. Ferdows et al. [32] examined the MHD biocon-

vection flow and thermal transfer of nanofluid as well as gyrotactic microorganisms which were studied by the side of an exponentially stretching layer. Alsenafi et al. [33] discussed a nonlinear shrinking/stretching sheet with unsteady nanofluid and bio-convective transportation features, as well as the mathematical analysis of the nanofilms' stagnation stream. Waqas et al. [34] investigated the impact of viscous dissipations via the numerical analysis of higher-order chemical reactions in electrical MHD nanofluids. Ayodeji et al. [35] explored the flow of nanofluid by bioconvection MHD via a flexible surface with velocity slip and viscous dissipation. Pal et al. [36] analyzed the influence of thermal radiation and gyrotactic microorganisms through an exponentially stretchable sheet in the presence of bioconvection MHD nanofluids. The bioconvection flow of visco-elastic nanofluids with magnetic motile and dipole microorganisms was examined by Alshomrani [37]. Zhao et al. [38] analyzed the suspensions of gyrotactic microorganisms with the heat of bioconvection which required immediate steadiness. The micropolar fluid mass and heat transformation through a perpendicular stretch sheet below the influence of motile microorganisms were investigated by Zadeh et al. [39]. Jawad et al. [40] studied the nanoparticles and motile microorganisms of the magnetohydrodynamics fluid through a permeable stretching sheet. Malek et al. [41] analyzed the unsteady free convection boundary-layer flow over a vertical surface Lie symmetry group. Lund et al. [42] expressed symmetrical solution and duality in the rotating 3D flow of hybrid nanofluid on exponentially shrinking sheet. Sindhu and Atangana [43] discussed the exponentiated inverse Weibull distribution and inverse power law and used them both in their reliability analysis. Shafiq et al. [44] analyzed the tangent hyperbolic nanofluid flow with Newtonian heating in a bioconvective MHD flow.

As we can observe, the literature has sought to address tackling the issue of the inclusion of nanoparticles which are responsible for enhancing the thermal conductivity of the base fluid. This can be helpful in the thermal management of industrial and technological processes as well as for heat exchangers and in microelectronics. However, the question of the sedimentation of nanoparticles may arise. Thus, the rising need for efficient thermal transportation can be achieved to cope with the issue of thermal balancing. This study explored the role of the bioconvection of microorganisms for the MHD flow of nanofluids due to the exponentially stretching sheet. Thermal radiation, chemical reaction, activation energy, and the Cattaneo–Christov heat flux were also considered. The results were numerically computed by using the Runge–Kutta method and coding the MATLAB scripts.

2. Problem Formulation

Here, the flow of nanofluids was undertaken when the sheet was stretched along the x axis with a stretching velocity of $U_w = U_0 e^{x/\ell}$. The flow was steady with the condition of incompressibility. The mild diffusion of the nanoparticles and microorganisms was set in the base fluid. The system of coordinates was chosen in such a way that the x axis aligned with the vertical plate and the y axis was perpendicular to the plate. The microorganisms moved independently with respect to the nano entities. The magnetic field of strength B_0 acted in the y direction. Thermal radiative and Cattaneo–Christov heat fluxes were considered. Bioconvection takes place due to the movement of microorganisms. The fluid velocity component for two-dimensional flow is u,v. The temperature is symbolized by T. The concentration of nanoparticles is C and that of microorganisms is N. The temperature $T_w(x)$, species concentration $C_w(x)$ and microorganism concentration $N_w(x)$ take a uniform value at the plate. In the far-off field, the volume of concentration, temperature, and microorganism concentration are presumed to be $C_\infty(x) = C_{\infty,0} + B_1 x$, $T_\infty(x) = T_{\infty,0} + A_1 x$, and $N_\infty(x) = N_{\infty,0} + C_1 x$, respectively, where A_1, B_1, and C_1 are constants and vary with the changing strength of stratification in the medium and $N_{\infty,0}$, $C_{\infty,0}$, and $T_{\infty,0}$ are the ambient of the microorganism concentration, the nanoparticle concentration, and the temperature at $x = 0$. The physical design of this problem is presented in Figure 1.

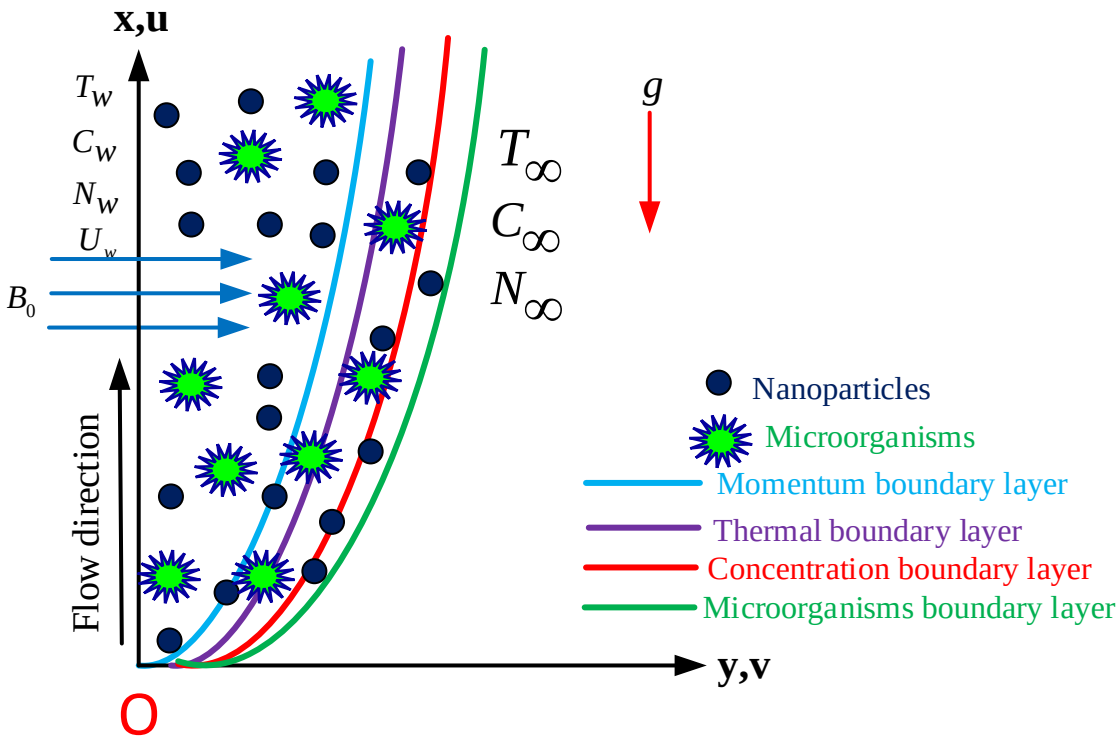

Figure 1. Geometry of the problem.

The governing equations of the fluid flow are given [45–47].
The Continuity Equation is as follows:

$$\frac{\partial u}{\partial x} + \frac{\partial v}{\partial y} = 0. \tag{1}$$

The Momentum equation [48] is as follows:

$$u\frac{\partial u}{\partial x} + v\frac{\partial u}{\partial y} = \nu\frac{\partial^2 u}{\partial y^2} - \frac{\sigma B_0^2}{\rho_f}u - \frac{\nu}{K_p'}u + \frac{1}{\rho_f}[g\beta\rho_f(1-C_\infty)(T-T_\infty) - g(\rho_p-\rho_f)(C-C_\infty) - g\gamma(\rho_m-\rho_f)(N-N_\infty)]. \tag{2}$$

The Energy equation [48] is as follows:

$$u\frac{\partial T}{\partial x} + v\frac{\partial T}{\partial y} + \lambda_2\left[u\frac{\partial u}{\partial x}\frac{\partial T}{\partial x} + v\frac{\partial v}{\partial y}\frac{\partial T}{\partial y} + u\frac{\partial v}{\partial x}\frac{\partial T}{\partial y} + v\frac{\partial u}{\partial y}\frac{\partial T}{\partial x} + 2uv\frac{\partial^2 T}{\partial x\partial y} + u^2\frac{\partial^2 T}{\partial x^2} + v^2\frac{\partial^2 T}{\partial y^2}\right] = \alpha\frac{\partial^2 T}{\partial y^2} - \frac{1}{\rho C_p}\frac{\partial q_r}{\partial y} + \frac{Q}{\rho C_p}(T-T_\infty) + \frac{\nu}{C_p}\left(\frac{\partial u}{\partial y}\right)^2 + \tau\left(D_B\frac{\partial C}{\partial y}\frac{\partial T}{\partial y} + \frac{D_T}{T_\infty}\left(\frac{\partial T}{\partial y}\right)^2\right). \tag{3}$$

Concentration equation [45]:

$$u\frac{\partial C}{\partial x} + v\frac{\partial C}{\partial y} = D_B\frac{\partial^2 C}{\partial y^2} + \frac{D_T}{T_\infty}\frac{\partial^2 T}{\partial y^2} - K_r(C-C_\infty) - K_r^2(C-C_\infty)\left(\frac{T}{T_\infty}\right)^n exp\left(\frac{-Ea}{kT}\right). \tag{4}$$

The Bioconvection equation [48] is as follows:

$$u\frac{\partial N}{\partial x} + v\frac{\partial N}{\partial y} + \frac{bW_c}{(C_w-C_\infty)}\frac{\partial}{\partial y}\left(N\frac{\partial C}{\partial y}\right) = D_m\frac{\partial^2 N}{\partial y^2}. \tag{5}$$

The boundary conditions are [45]:

$$\left.\begin{array}{r} u = U_w(x) = U_0 e^{x/\ell}, v = 0,\ T - T_w = 0,\ C - C_w = 0,\ N - N_w = 0,\ as\ y = 0, \\ u \to 0,\ T \to T_\infty,\ C \to C_\infty,\ N \to N_\infty,\ as\ y \to \infty. \end{array}\right\} \quad (6)$$

Using the Roseland approximation for radiation, the radiative heat flux q_r is given by [49]

$$q_r = \frac{-4\sigma^*}{3k^*}\frac{\partial T^4}{\partial y}, \quad (7)$$

where σ^* is the Stefan–Boltzman constant and k* is the coefficient of mean absorption. We assume that the temperature difference within the flow is sufficiently small. The expression for T^4 we obtain using the Taylor series in powers of $(T - T_\infty)$ when higher-order terms are neglected, is:

$$T^4 \approx 4T_\infty^3 T - 3T_\infty^4,$$

$$q_r = \frac{-16\sigma^* T_\infty^3}{3k^*}\frac{\partial T}{\partial y},\ then\ \frac{\partial q_r}{\partial y} = \frac{-16\sigma^* T_\infty^3}{3k^*}\frac{\partial^2 T}{\partial y^2}. \quad (8)$$

The stream function is:

$$u = \frac{\partial \psi}{\partial y},\ v = -\frac{\partial \psi}{\partial x}. \quad (9)$$

Considering the similarity transformation [45]:

$$\left.\begin{array}{r} \xi = y\sqrt{\frac{U_0}{2\nu\ell}}e^{\frac{x}{2\ell}},\ u = U_0 e^{\frac{x}{\ell}} f'(\xi),\ vs. = -\sqrt{\frac{\nu U_0}{2\ell}}e^{\frac{x}{2\ell}}[f(\xi) + \xi f'(\xi)], \\ T = T_\infty + T_0 e^{\frac{x}{2\ell}}\theta(\xi), C = C_\infty + C_0 e^{\frac{x}{2\ell}}\phi(\xi), N = N_\infty + N_0 e^{\frac{x}{2\ell}}\chi(\xi), B = B_0 e^{\frac{x}{2\ell}}. \end{array}\right\} \quad (10)$$

In view of the above appropriate relations Equation (1) is satisfied and Equations (2)–(5), respectively, become:

$$f'''(\xi) + f(\xi)f''(\xi) - 2(f')^2(\xi) - (M + \frac{1}{K_p})f'(\xi) + \lambda(\theta(\xi) - Nr\phi(\xi) - Rb\chi(\xi)) = 0, \quad (11)$$

$$\frac{1}{Pr}(1 + \frac{4}{3}Rd)\theta''(\xi) + f(\xi)\theta'(\xi) - f'(\xi)\theta(\xi) + S\theta(\xi) + Ec(f'')^2(\xi) + Nb\theta'(\xi)\phi'(\xi) + Nt(\theta')^2(\xi) - \delta_2[3f'^2(\xi)\theta(\xi) - 3f(\xi)f'(\xi)\theta'(\xi) - \theta(\xi)f(\xi)f''(\xi) + (f)^2(\xi)\theta''(\xi)] = 0, \quad (12)$$

$$\phi''(\xi) + Sc[f(\xi)\phi'(\xi) - f'(\xi)\phi(\xi) - Cr\phi(\xi) - \sigma_m\phi(\xi)(1 + \delta\theta(\xi))^n exp(\frac{-E}{1 + \delta\theta(\xi)})] + \frac{Nt}{Nb}\theta'' = 0, \quad (13)$$

$$\chi''(\xi) + LbPrf(\xi)\chi'(\xi) - LbPrf'(\xi)\chi(\xi) - Pe(\sigma_1\phi''(\xi) + \chi(\xi)\phi''(\xi) + \chi'(\xi)\phi'(\xi)) = 0. \quad (14)$$

The boundary conditions (6) are reduced to the following form:

$$\left.\begin{array}{r} f'(0) = 1,\ f(0) = 0,\ \theta(0) = 1,\ \phi(0) = 1,\ \chi(0) = 1,\ at\ \ \xi = 0, \\ f'(\infty) \to 0,\ \theta(\infty) \to 0,\ \phi(\infty) \to 0,\ \chi(\infty) \to 0\ \ as\ \xi \to \infty. \end{array}\right\} \quad (15)$$

The associated parameters, as they appear in the modeled problem, are:
$M = \frac{2\sigma B_0^2 \ell}{\rho_f U_w}$, $Pr = \frac{\nu}{\alpha}$, $K_p = \frac{2\nu\ell}{K_p' U_w}$, $\lambda = \frac{(1-C_\infty)\beta g(T_w - T_\infty)2\ell}{U_w^2}$, $Nr = \frac{(\rho_p - \rho_f)(C_w - C_\infty)}{\beta(1-C_\infty)\rho_f(T_w - T_\infty)}$, $\tau =$

$\frac{(\rho C)_p}{(\rho C)_f}$
$Rb = \frac{(\rho_m-\rho_f)\gamma(N_w-N_\infty)}{\rho_f(1-C_\infty)\beta(T_w-T_\infty)}$, $S = \frac{2\ell Q}{\rho_f U_w C_p}$, $Ec = \frac{U_w^2}{(T_w-T_\infty)C_p}$, $Nt = \frac{\tau D_T(T_w-T_\infty)}{\nu T_\infty}$, $Nb = \frac{\tau D_B(C_w-C_\infty)}{\nu}$,
$\delta_2 = \frac{\lambda_2 U_w}{2\ell}$, $Cr = \frac{2\ell K_r}{U_w}$, $\sigma_m = \frac{2K_r^2\ell}{U_w}$, $\delta = \frac{(T_w-T_\infty)}{T_\infty}$, $E = \frac{Ea}{kT_\infty}$, $Rd = \frac{4\sigma^* T_\infty^3}{k^*\kappa}$, $Sc = \frac{\nu}{D_B}$,
$\alpha = \frac{\kappa}{\rho_f C_p}$, $Lb = \frac{\alpha}{D_m}$, $Pe = \frac{bW_c}{D_m}$, $\sigma_1 = \frac{N_\infty}{N_w-N_\infty}$.

The shearing stress at the surface of the wall τ_w is given by

$$\tau_w = -\mu\left[\frac{\partial u}{\partial y}\right]_{y=0} = -\mu\left[U_0 e^{\frac{3x}{2\ell}}\sqrt{\frac{U_0}{2\nu\ell}}f''(0)\right], \tag{16}$$

where μ is the coefficient of viscosity. The skin friction coefficient is defined as

$$C_f = \frac{2\tau_w}{\rho_f U_w^2}, \tag{17}$$

using Equation (16) in Equation (17), we obtain:

$$\frac{C_f Re_x^{\frac{1}{2}}}{\sqrt{2}} = -f''(0). \tag{18}$$

The heat transfer rate at the surface of the wall is given by

$$q_w = -k\left[\frac{\partial T}{\partial y}\right]_{y=0} = -\kappa\left[(T_w - T_\infty)e^{\frac{x}{2\ell}}\sqrt{\frac{U_0}{2\nu\ell}}\,\theta'(0)\right], \tag{19}$$

where κ is the thermal conductivity of the fluid. The Nusselt number is defined as

$$Nu_x = -\frac{\sqrt{2}\ell}{\kappa}\frac{q_w}{(T_w - T_\infty)}, \tag{20}$$

using Equation (19) in Equation (20), we obtain:

$$Nu_x Re_x^{-\frac{1}{2}} = -\theta'(0). \tag{21}$$

The mass flux at the surface of the wall is given by

$$q_m = -D_B\left[\frac{\partial C}{\partial y}\right]_{y=0} = -D_B\left[(C_w - C_\infty)e^{\frac{x}{2\ell}}\sqrt{\frac{U_0}{2\nu\ell}}\,\phi'(0)\right], \tag{22}$$

where D_B is the Brownian diffusivity. The Sherwood number is defined as

$$Sh_x = -\frac{\sqrt{2}\ell}{D_B}\frac{q_m}{(C_w - C_\infty)}, \tag{23}$$

using Equation (22) in Equation (23), we obtain:

$$Sh_x Re_x^{-\frac{1}{2}} = -\phi'(0). \tag{24}$$

The density of the motile microorganisms' density at the surface of the wall is given by

$$q_n = -D_m\left[\frac{\partial N}{\partial y}\right]_{y=0} = -D_m\left[(N_w - N_\infty)e^{\frac{x}{2\ell}}\sqrt{\frac{a_0}{2\nu\ell}}\,\chi'(0)\right], \tag{25}$$

where D_m is the microorganisms' diffusion coefficient. The density of motile microorganisms is defined as

$$Nn_x = -\frac{\sqrt{2}\ell}{D_m}\frac{q_n}{(N_w - N_\infty)}, \tag{26}$$

using Equation (25) in Equation (26), we obtain:

$$Nn_x Re_x^{-\frac{1}{2}} = -\chi'(0). \tag{27}$$

where Re_x represents the local Reynolds number and it is defined as $Re_x = \frac{U_w \ell}{\nu}$.

3. Solution Procedure

The resulting set of ODEs (11–14) with the boundary conditions (15) constitutes a highly nonlinear boundary value problem. It seems difficult to find any closed-form solution. It was treated numerically by hiring the Runge–Kutta method, along with the shooting technique method. The implementation of the scheme requires first-order differential equations to be acquired as follows:

$w_1' = w_2$,
$w_2' = w_3$,
$w_3' = (-1)[w_1 w_3 - 2w_2^2 - (M + \frac{1}{K_p})w_2 + \lambda(w_4 - Nr\, w_6 - Rb\, w_8)]$,
$w_4' = w_5$,
$w_5' = (-Pr)(1 + \frac{4}{3}Rd)^{-1}[w_1 w_5 - w_2 w_4 + S w_4 + Ec\, w_3^2 + Nb w_5 w_7 + Nt w_5^2 - \delta_2(3w_2^2 w_4 - 3w_1 w_2 w_5 - w_4 w_1 w_3 + w_1^2 w_5')]$,
$w_6' = w_7$,
$w_7' = (-Sc)[w_1 w_7 - w_2 w_6 - Cr w_6 - \sigma_m w_6(1 + \delta w_4)^n exp(-\frac{E}{1+\delta w_4})] - \frac{Nt}{Nb}w_5'$,
$w_8' = w_9$,
$w_9' = (-1)[PrLb w_1 w_9 - PrLb w_2 w_8 - Pe[w_7'(w_8 + \sigma_1) + w_7 w_9]]$,
along with the boundary conditions:
$w_2 = 1,\ w_1 = 0, w_4 = 1,\ w_6 = 1,\ w_8 = 1,\ at\ \xi = 0$,
$w_2 \to 0,\ w_4 \to 0,\ w_6 \to 0,\ w_8 \to 0\ as\ \xi \to \infty$.

This system of first-order differential equations were coded in the MatLab environment and computations were performed for the varying values of influential parameters.

4. Analysis of Results and Discussion

This segment presents the results as enumerated from the aforementioned coding for the varying behaviors of fluid velocity, temperature, skin friction factor, concentration function, bioconvection function, Nusselt number, motile microorganisms' number, and Sherwood number, which are observed and tabulated for the suitable ranges of sundry parameters. The estimates of the present findings are computed by putting the values of the involved parameter to be fixed as: Cr = 0.2; M = 1.0; Rd = 0.2; Ec = 0.1; S = 0.10; Pr = 1.0; Sc = 0.22; K_p = 100; λ = 0.2; Nr = 0.03; Rb = 0.2; Nb = 0.1; Nt = 0.1; δ_2 = 0.1; σ_m = 0.3; E = 0.6; n = 0.5; δ = 0.3; Lb = 1.8; Pe = 0.1; σ_1 = 0.3. The validation of the present numeric outputs was achieved through their acceptable comparison with previous studies [49,50]. Tables 1 and 2 exhibit the comparative data for the skin friction factor $-f''(0)$ and Nusselt number $-\theta'(0)$. Table 3 presents the results for the Sherwood number $-\phi'(0)$ and Table 4 for the density of motile microorganisms $-\chi'(0)$. The graphical outputs are mentioned in Figures 2–11. From Figure 2a, the variation of the velocity in the reducing pattern is noticed against exceeding inputs of magnetic parameters M. The growing strength of M means a larger resistive force to the flow. The resistive Lorentz force comes into play with the interaction magnetic and electric fields. This result is in concurrence with [45]. The supporting role of the porosity parameter K_p on the velocity $f'(\xi)$ is depicted in Figure 2b. The parameter K_p is reciprocal to the viscosity and directly proportional to the permeability of the medium. The larger values of K_p mean enhanced permeability which gives rise to the

flow and enhances the velocity curve directly increasingly with K_p. The mixed convection parameter helps to improve the flow speed $f'(\xi)$ as noticed in Figure 3a. The convection provides an increased buoyancy effect to the flow with the temperature difference and density variation. This phenomenon accelerates the flow. The growing buoyancy ratio parameter Nr diminishes the fluid velocity $f^{'}$ (see Figure 3b). Figure 4a delineates the temperature curve to increase with the magnetic parameter M. This is because the flow is slowed and kinetic energy is transferred to the heat energy and enhances the temperature of the fluid. Figure 4b exhibits the reducing patterns of temperature $\theta(\xi)$ concerning the parameter λ. Figure 5a exhibits the impact of the Prandtl number Pr over the temperature profile $\theta(\xi)$. It can be noticed that the thickness of the thermal boundary layer is minimized by the growth in the amount of Prandtl number. The increases in the radiation parameter Rd lead to enhanced temperature $\theta(\xi)$ due to the incremented radiative heat transport, as depicted in Figure 5b. Figure 6a presents the influence on the temperature profile $\theta(\xi)$ of the source parameter S. The temperature profile $\theta(\xi)$ is noticeably enhanced as the source parameter S increases. Figure 6b sketches the reducing temperature $\theta(\xi)$ due to enhanced values of the thermal relaxation parameter. Figure 7a presents the rising behavior of $\theta(\xi)$ with the enhanced Brownian motion of nano entities to be responsible for improved thermal distribution. The thermophoretic effects which cause the nano entities to move from warm regions to colder ones also increased the temperature, as shown in Figure 7b. Figure 8a demonstrates the reducing behavior of the concentration function ϕ as inversely related to the Schmidt number. The larger Schmidt number means a smaller diffusion coefficient and hence, results in the reduction in $\phi(\xi)$. The chemical reaction parameter Cr also causes a decrement in $\phi(\xi)$, as displayed in Figure 8b. This is because the faster chemical reaction reduces the concentration. The reaction rate parameter σ_m notably decreases the concentration, as can be seen in Figure 9a. However, the activation energy parameter E enhances the concentration function $\phi(\xi)$ as seen in Figure 9b. The effects of the bioconvection Rayleigh number Rb on the density of the motile microorganisms $\chi(\xi)$ in nanofluid were shown in Figure 10a. The density of the motile microorganisms $\chi(\xi)$ increases as Rb increases. The impact of the bioconvection Lewis number Lb on the microorganism $\chi(\xi)$ is inspected in Figure 10b. The tense product exhibits how the motility distribution reduces because of the effect of Lb because of the lower dispersion of microorganisms. Usually, we can say that Lb assumes a more grounded job to decline the $\chi(\xi)$ of nanofluid. Figure 11a recommends the effect of the Peclet number Pe on motile $\chi(\xi)$. The advanced estimations of Pe compared to the motile dissemination were chosen because of the diminishing microorganism $\chi(\xi)$. Figure 11b displays the effect of the difference factor of the microorganism concentration σ_1 on the motile thickness of the microorganism. It can be seen in the figure that both the limit of the layer thickness of the microorganism and the thickness decreases for expanding values of σ_1.

Table 1. Comparison of $C_f Re_x^{\frac{1}{2}}$ (skin friction coefficient) $-f''(0)$ with the variation of the magnetic parameter M when K_p, λ, Nr, Rb = 0.

M	Kameswaran et al. [46]	Our Results
0	1.281809	1.281816
1	1.629178	1.629178
2	1.912620	1.912620
3	2.158736	2.158736
5	2.581130	2.581130
10	3.415290	3.415290

Table 2. Comparison of $Nu_x Re_x^{-\frac{1}{2}}$ $(-\theta'(0))$ values for the Prandtl number Pr, radiation number Rd, magnetic parameter M and other parameter K_p, λ, Nr, Rb, S, Ec, Nb, Nt, $\delta_2 = 0$.

Pr	Rd	M	Ishak [47]	Mukhopadhyay [51]	Our Results
1	0	0	0.9548	0.9547	0.9548
2			1.4715	1.4714	1.4715
3			1.8691	1.8691	1.8691
5			2.5001	2.5001	2.5001
10			3.6604	3.6603	3.6604
1		1	0.8611	0.8610	0.8615
	0.5	0			0.6775
	1		0.5312	0.5311	0.5313
		1	0.4505	0.4503	0.4620
2	0.5	0		1.0734	1.0735
	1			0.8626	0.8629
3	0.5			1.3807	1.3808
	1			1.1213	1.1214

Table 3. Influence of various physical parameters over the Sherwood number $Sh_x Re_x^{-\frac{1}{2}} = -\phi'(0)$.

Sc	Cr	σ_m	Nt	Nb	n	E	Sh_x
0.3							0.4789
0.5							0.6808
0.7							0.8504
0.9							0.9998
	0.2						0.2119
	0.3						0.2341
	0.4						0.2548
	0.5						0.2743
		0.2					0.1937
		0.4					0.2291
		0.6					0.2610
		0.8					0.2901
			0.1				0.2119
			0.2				0.1490
			0.3				0.1084
			0.4				0.0596
				0.1			0.2119
				0.2			0.2474
				0.3			0.2595
				0.4			0.2656
					1.0		0.2144
					4.0		0.2264
					7.0		0.2410
					10.0		0.2588
						0.3	0.2119
						0.9	0.1882
						1.5	0.2738
						2.0	0.1664

Table 4. Influence of various physical parameters over the density of motile microorganisms $Nn_xRe_x^{-\frac{1}{2}} = -\chi'(0)$.

Pe	Lb	σ_1	Pr	Nn_x
0.1				1.2508
0.3				1.2726
0.5				1.2947
0.7				1.3172
	1.0			0.6965
	1.5			0.9985
	2.0			1.2508
	2.5			1.4714
		0.1		1.2502
		0.3		1.2508
		0.6		1.2518
		0.9		1.2528
			1.1	1.3436
			1.2	1.4314
			1.3	1.5149
			1.4	1.5946

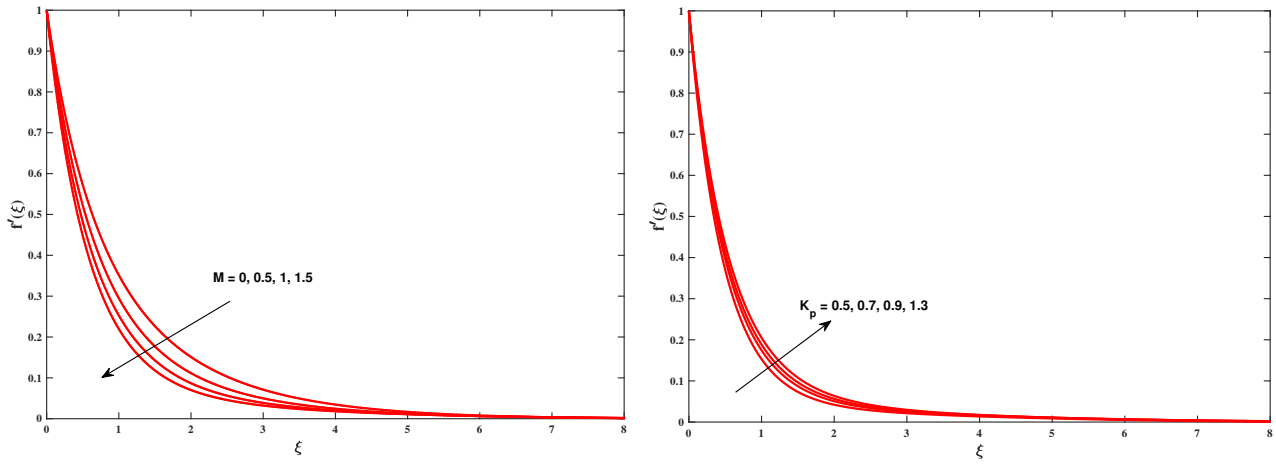

(**a**) (**b**)

Figure 2. Sketch of f' for different inputs of (**a**) for M and (**b**) for K_p.

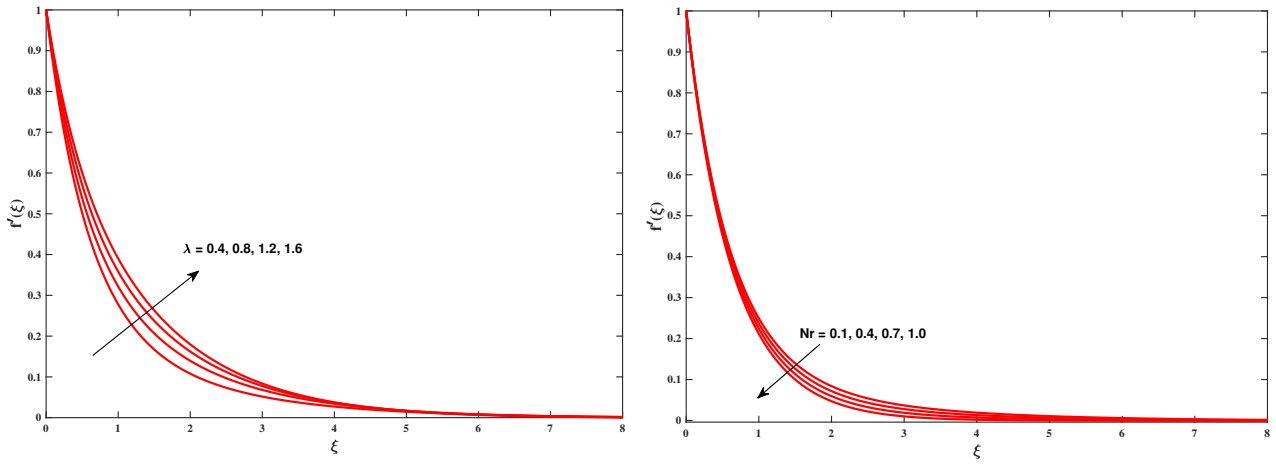

(**a**) (**b**)

Figure 3. Sketch of f' for different inputs of (**a**) for λ and (**b**) for Nr.

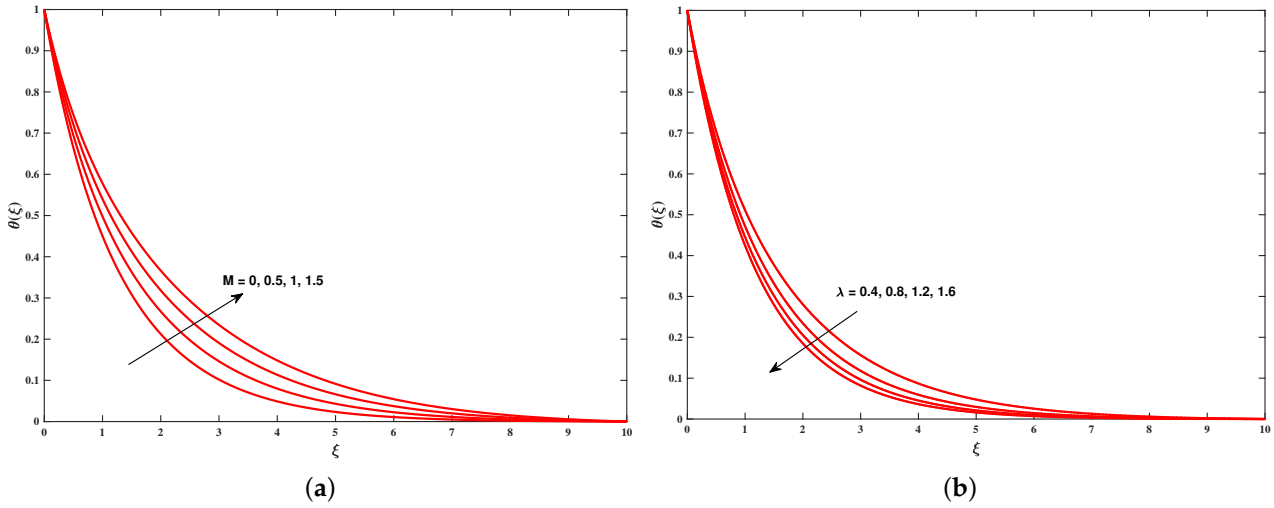

Figure 4. Sketch of θ for different inputs of (**a**) for M and (**b**) for λ.

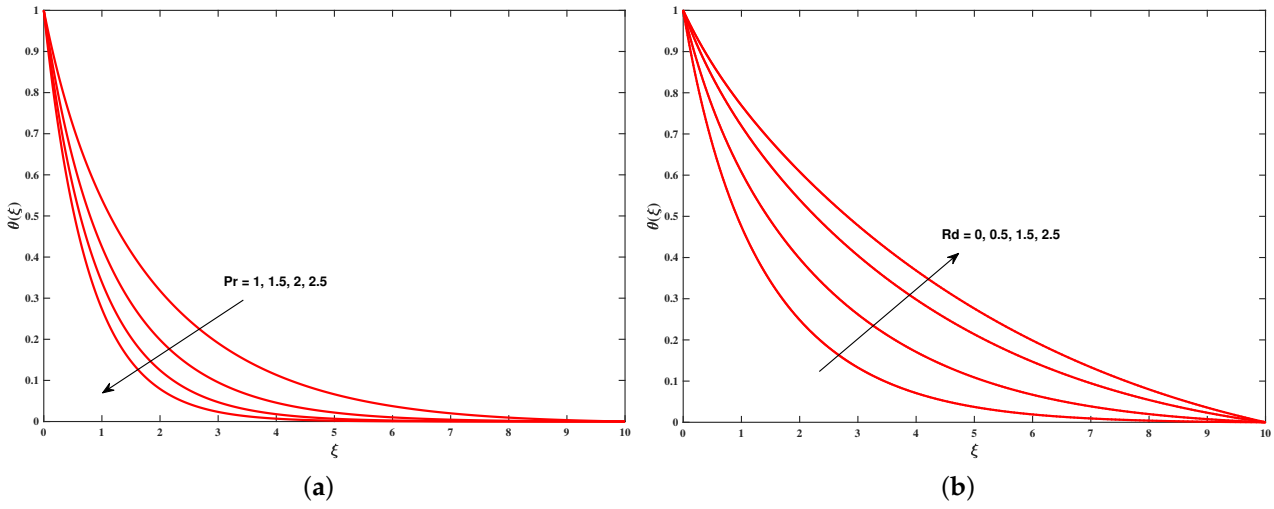

Figure 5. Sketch of θ for different inputs of (**a**) for Pr and (**b**) for Rd.

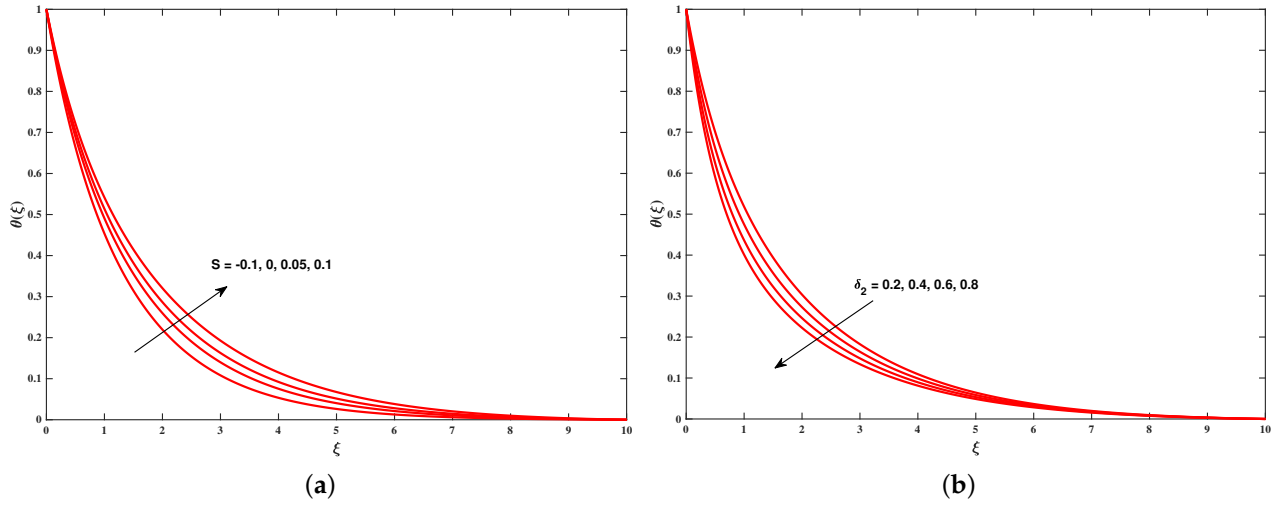

Figure 6. Sketch of θ for different inputs of (**a**) for S and (**b**) for δ_2.

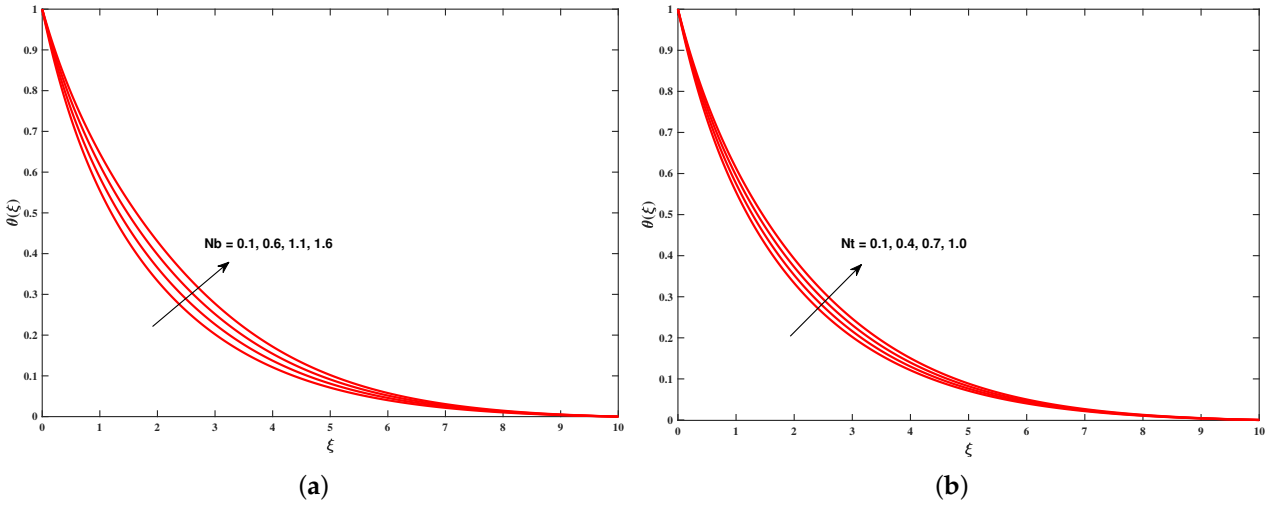

Figure 7. Sketch of θ for different inputs of (**a**) for Nb and (**b**) for Nt.

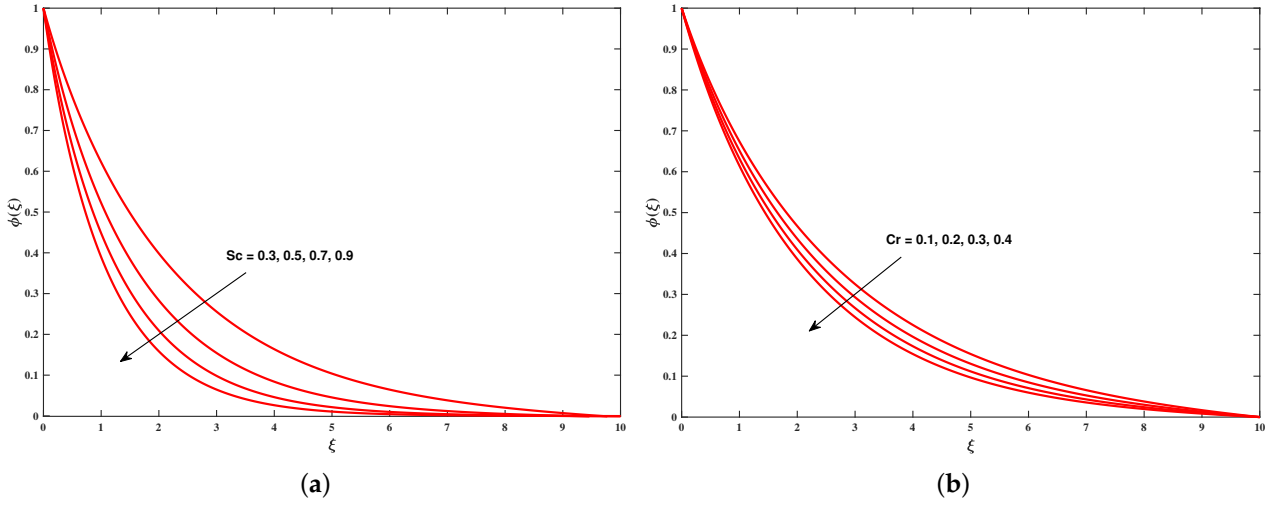

Figure 8. Sketch of ϕ for different inputs of (**a**) for Sc and (**b**) for Cr.

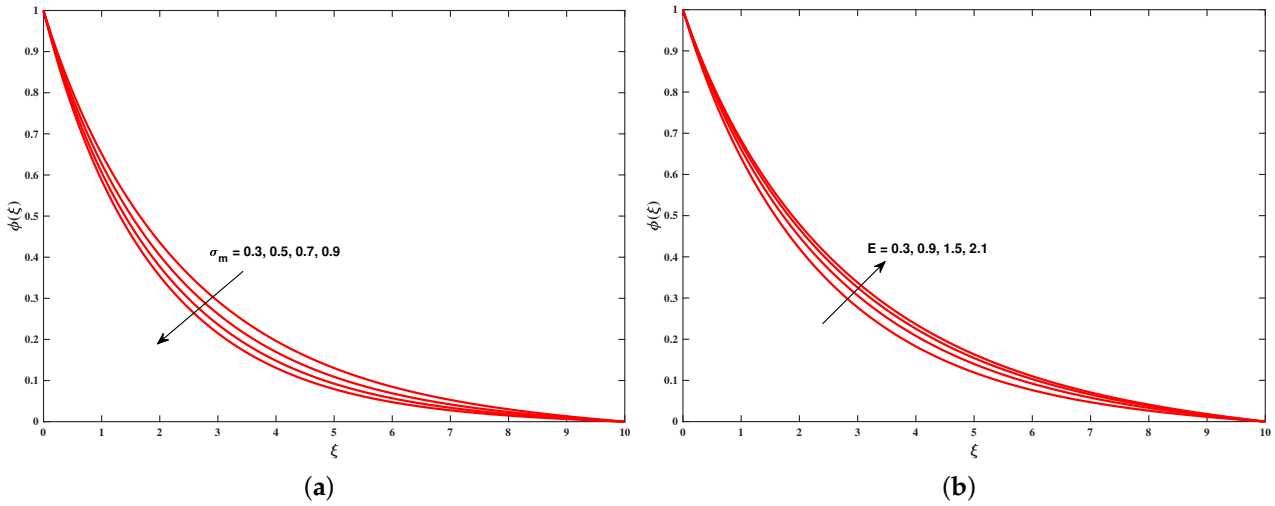

Figure 9. Sketch of ϕ for different inputs of (**a**) for σ_m and (**b**) for E.

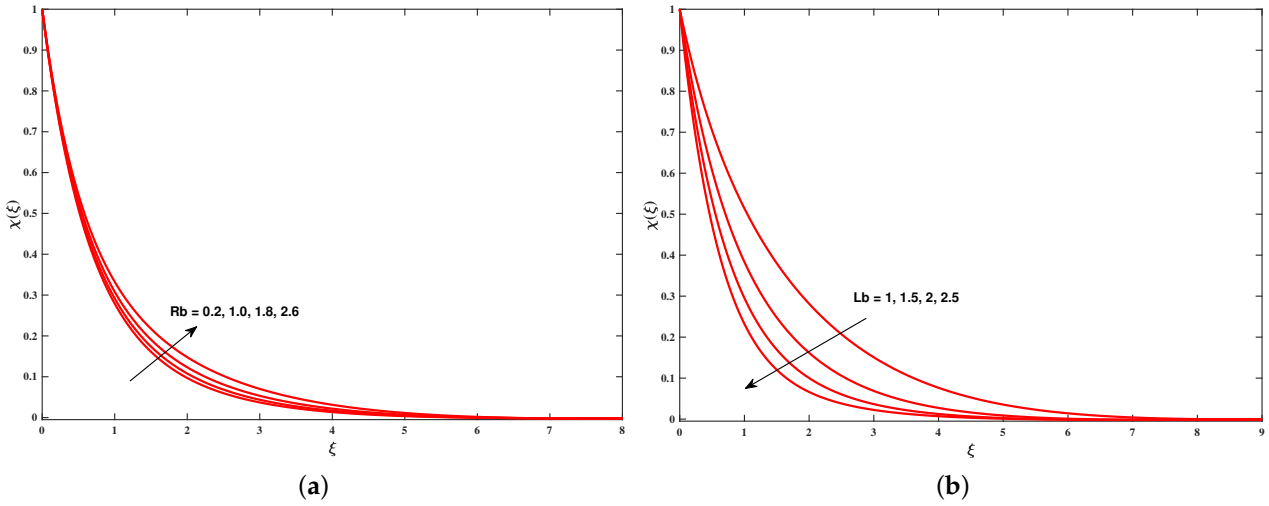

Figure 10. Sketch of χ for different inputs of (**a**) for Rb and (**b**) for Lb.

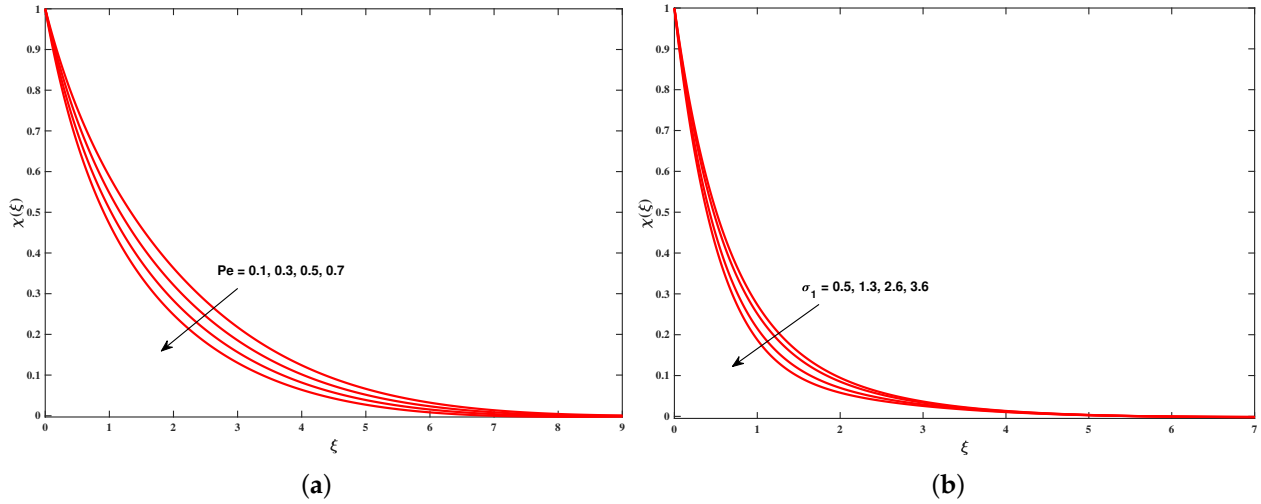

Figure 11. Sketch of χ for different inputs of (**a**) for Pe and (**b**) for σ_1.

5. Conclusions

Numerical and theoretical analyses of microorganisms and their activation energy effects were performed for the flow of nanofluids due to the exponentially stretching sheet. Cattaneo–Christov heat diffusion and thermal radiation fluxes were considered. Furthermore, the validation of important findings and results were deliberated. The satisfactory concurrence was observed when results were compared with the existing literature. The controlling parameters were varied in appropriate ranges to elucidate their impacts on temperature, velocity, microorganisms' distribution, and nanoparticle volume fraction. Some salient outputs are summarized:

- The velocity profile was escalated for the mixed convection parameter and porosity parameter while it was depressed for the buoyancy ratio parameter and magnetic field parameter.
- The fluid temperature was increased for the magnetic parameter, radiation parameter, heat source parameter, thermophoresis, and Brownian motion parameters while it was decreasing against the Prandtl number, mixed convection parameter, and thermal relaxation parameter.
- The concentration of nanoparticles was reduced due to the Schmidt number, chemical reaction parameter, and reaction rate parameter, while it was boosted with the activation energy parameter.

- The density of the motile microorganism is a decreasing function of the Peclet number, bioconvection Lewis number, and bioconvection difference parameter while it is increasing for the bioconvection Rayleigh number.
- Nanoparticles slip parameters Nb and Nt showed an increment in the temperature profile. Furthermore, the parameters due to bioconvection had a significant influence on the flow of fluid.
- Furthermore, a study can be carried out with an increment in the volume fraction, and non-Newtonian base fluid, and hybrid nanofluids.

Author Contributions: Conceptualization, M.I.A.; Formal analysis, B.A.; Funding acquisition, T.S.; Investigation, M.I.A.; Methodology, N.S.; Project administration, T.S.; Resources, J.R.; Software, B.A.; Validation, S.H.; Visualization, S.H.; Writing — original draft, N.S.; Writing — review & editing, J.R. All authors have read and agreed to the published version of the manuscript.

Funding: This research was funded by King Mongkut's University of Technology North Bangkok. Contract no. KMUTNB-63-KNOW-19.

Institutional Review Board Statement: Not applicable.

Informed Consent Statement: Not applicable.

Data Availability Statement: Not applicable.

Acknowledgments: The authors are grateful to the University of Management and Technology Lahore, Pakistan, for facilitating and supporting this research study.

Conflicts of Interest: The authors declare no conflict of interest.

Nomenclature

Symbol	Explanation	Symbol	Explanation
B_0	Coefficient of magnetic field	C	Concentration of nanoparticles
C_p	Specific heat capacity	N	Concentration of microorganisms
Nt	Thermopherosis parameter	(x, y)	Cartesian coordinates
Cr	Chemical reaction parameter	(u, v)	Velocity components along (x, y) axes
$K_p^{'}$	Permeability of the fluid	ξ	Similarity variable
Q	Dimensional heat source	ϕ	Dimensionless concentration
q_r	Radiative heat flux	ρ	Density
U_w	Stretching velocity	μ	Dynamic viscosity of the fluid
D_B	Brownian diffusivity	σ	Electrical conductivity
K_p	Porosity parameter	ψ	Stream function
Rd	Radiation parameter	δ	Temperature distinction parameter
Sc	Schmidt number	λ	Mixed convection parameter
Ec	Eckert number	ν	Kinematic viscosity
Pr	Prandtl number	θ	Dimensionless temperature
S	Source parameter	χ	Dimensionless microorganism factor
M	Magnetic field parameter	ρ_f	Density of nanofluid
Nr	Buoyancy ratio parameter	ρ_m	Density of microorganism particles
Rb	Bioconvection Rayleigh number	ρ_p	Density of nanoparticles
Nb	Brownian motion parameter	κ	Thermal conductivity
n	Fitted rate constant parameter	α	Thermal diffusivity
K_r^2	Chemical reaction rate constant	β	Volumetric coefficient of thermal expansion
E	Dimensional activation energy	γ	Average volume of microorganism
Lb	Bioconvection Lewis number	λ_2	Relaxation time of the heat flux
D_T	Thermophoretic diffusion coefficient	δ_2	Thermal relaxation parameter
W_c	Maximum cell swimming speed	σ_m	Dimensionless reaction rate

Symbol	Explanation	Symbol	Explanation
D_m	Microorganism diffusion coefficient	σ_1	Bioconvection difference parameter
K_r	Rate of chemical reaction	w	Condition at the wall
Pe	Peclet number	∞	The outer edge of boundary layer
g	Gravity	τ	Heat capacity ratio
T	Temperature	Sh_x	Local Sherwood Number
σ^*	Stefan Boltzman constant	Nu_x	Local Nusselt number
C_f	Local skin friction number	Re_x	Local Reynolds number

References

1. Hsiao, K.L. Micropolar nanofluid flow with MHD and viscous dissipation effects towards a stretching sheet with multimedia feature. *Int. J. Heat Mass Transf.* **2017**, *112*, 983–990. [CrossRef]
2. Ali, B.; Rasool, G.; Hussain, S.; Baleanu, D.; Bano, S. Finite element study of magnetohydrodynamics (MHD) and activation energy in Darcy-Forchheimer rotating flow of Casson Carreau nanofluid. *Processes* **2020**, *8*, 1185. [CrossRef]
3. Abdal, S.; Ali, B.; Younas, S.; Ali, L.; Mariam, A. Thermo-diffusion and multislip effects on MHD mixed convection unsteady flow of micropolar nanofluid over a shrinking/stretching sheet with radiation in the presence of heat source. *Symmetry* **2020**, *12*, 49. [CrossRef]
4. Daniel, Y.S.; Aziz, Z.A.; Ismail, Z.; Bahar, A.; Salah, F. Slip role for unsteady MHD mixed convection of nanofluid over stretching sheet with thermal radiation and electric field. *Indian J. Phys.* **2020**, *94*, 195–207. [CrossRef]
5. Kumar, M.A.; Reddy, Y.D.; Rao, V.S.; Goud, B.S. Thermal radiation impact on MHD heat transfer natural convective nano fluid flow over an impulsively started vertical plate. *Case Stud. Therm. Eng.* **2021**, *24*, 100826. [CrossRef]
6. Abdel-Rahman Rashed, G.M. Entropy and radiation on a pipe MHD flow with variable viscosity. *Heat Transf.* **2021**, *50*, 1697–1711. [CrossRef]
7. Poply, V.; Singh, P.; Yadav, A.K. Stability analysis of MHD outer velocity flow on a stretching cylinder. *Alex. Eng. J.* **2018**, *57*, 2077–2083. [CrossRef]
8. Dawar, A.; Shah, Z.; Tassaddiq, A.; Islam, S.; Kumam, P. Joule heating in magnetohydrodynamic micropolar boundary layer flow past a stretching sheet with chemical reaction and microstructural slip. *Case Stud. Therm. Eng.* **2021**, *25*, 100870. [CrossRef]
9. Khan, S.A.; Nie, Y.; Ali, B. Multiple slip effects on MHD unsteady viscoelastic nano-fluid flow over a permeable stretching sheet with radiation using the finite element method. *SN Appl. Sci.* **2020**, *2*, 1–14. [CrossRef]
10. Jabeen, K.; Mushtaq, M.; Akram Muntazir, R.M. Analysis of MHD fluids around a linearly stretching sheet in porous media with thermophoresis, radiation, and chemical reaction. *Math. Probl. Eng.* **2020**, *2020*, 9685482. [CrossRef]
11. Choi, S.U.S.; Eastman, J.A. Enhancing thermal conductivity of fluids with nanoparticles. In Proceedings of the ASME International Mechanical Engineering Congress and Exposisition, American Society of Mechanical Engineers, San Francisco, FL, USA, 12–17 November 1995; Volume 66, pp. 99–105.
12. Gopal, D.; Saleem, S.; Jagadha, S.; Ahmad, F.; Almatroud, A.O.; Kishan, N. Numerical analysis of higher order chemical reaction on electrically MHD nanofluid under influence of viscous dissipation. *Alex. Eng. J.* **2021**, *60*, 1861–1871. [CrossRef]
13. Ghasemi, S.E.; Hatami, M. Solar radiation effects on MHD stagnation point flow and heat transfer of a nanofluid over a stretching sheet. *Case Stud. Therm. Eng.* **2021**, *25*, 100898. [CrossRef]
14. Krishna, M.V.; Ahamad, N.A.; Chamkha, A.J. Radiation absorption on MHD convective flow of nanofluids through vertically travelling absorbent plate. *Ain Shams Eng. J.* **2021**, *12*, 3043–3056. [CrossRef]
15. Abbas, N.; Nadeem, S.; Saleem, A.; Malik, M.Y.; Issakhov, A.; Alharbi, F.M. Models base study of inclined MHD of hybrid nanofluid flow over nonlinear stretching cylinder. *Chin. J. Phys.* **2021**, *69*, 109–117. [CrossRef]
16. Zainal, N.A.; Nazar, R.; Naganthran, K.; Pop, I. Stability analysis of MHD hybrid nanofluid flow over a stretching/shrinking sheet with quadratic velocity. *Alex. Eng. J.* **2021**, *60*, 915–926. [CrossRef]
17. Sreedevi, P.; Reddy, P.S.; Chamkha, A. Heat and mass transfer analysis of unsteady hybrid nanofluid flow over a stretching sheet with thermal radiation. *SN Appl. Sci.* **2020**, *2*, 1–15. [CrossRef]
18. Shoaib, M.; Raja, M.A.Z.; Sabir, M.T.; Islam, S.; Shah, Z.; Kumam, P.; Alrabaiah, H. Numerical investigation for rotating flow of MHD hybrid nanofluid with thermal radiation over a stretching sheet. *Sci. Rep.* **2020**, *10*, 1–15. [CrossRef]
19. Narender, G.; Govardhan, K.; Sarma, G.S. Numerical study of radiative magnetohydrodynamics viscous nanofluid due to convective stretching sheet with the chemical reaction effect. *Iraqi J. Sci.* **2020**, *61*, 1733–1744. [CrossRef]
20. Rashid, U.; Baleanu, D.; Iqbal, A.; Abbas, M. Shape effect of nanosize particles on magnetohydrodynamic nanofluid flow and heat transfer over a stretching sheet with entropy generation. *Entropy* **2020**, *22*, 1171. [CrossRef]
21. Crane, L.J. Flow past a stretching plate. *Z. Für Angew. Math. Und Phys. ZAMP* **1970**, *21*, 645–647. [CrossRef]
22. Gupta, P.S.; Gupta, A.S. Heat and mass transfer on a stretching sheet with suction or blowing. *Can. J. Chem. Eng.* **1977**, *55*, 744–746. [CrossRef]
23. Yasmin, A.; Ali, K.; Ashraf, M. Study of heat and mass transfer in MHD flow of micropolar fluid over a curved stretching sheet. *Sci. Rep.* **2020**, *10*, 1–11.

24. Swain, B.K.; Parida, B.C.; Kar, S.; Senapati, N. Viscous dissipation and joule heating effect on MHD flow and heat transfer past a stretching sheet embedded in a porous medium. *Heliyon* **2020**, *6*, e05338. [CrossRef]
25. Reddy, Y.D.; Rao, V.S.; Kumar, M.A. Effect of heat generation/absorption on MHD copper-water nanofluid flow over a non-linear stretching/shrinking sheet. *AIP Conf. Proc.* **2020**, *2246*, 020017.
26. Singh, J.; Mahabaleshwar, U.S.; Bognár, G. Mass transpiration in nonlinear MHD flow due to porous stretching sheet. *Sci. Rep.* **2019**, *9*, 1–15.
27. Murtaza, M.G.; Tzirtzilakis, E.E.; Ferdows, M. A note on MHD flow and heat transfer over a curved stretching sheet by considering variable thermal conductivity. *Int. J. Math. Comput. Sci.* **2018**, *12*, 38–42.
28. Narsingani, L.S. A numerical solution for magnetohydrodynamic stagnation-point flow towards a stretching sheet. *Turk. J. Comput. Math. Educ. (TURCOMAT)* **2021**, *12*, 6450–6457.
29. Ali, B.; Naqvi, R.A.; Nie, Y.; Khan, S.A.; Sadiq, M.T.; Rehman, A.U.; Abdal, S. Variable viscosity effects on unsteady MHD an axisymmetric nanofluid flow over a stretching surface with thermo-diffusion: Fem approach. *Symmetry* **2020**, *12*, 234. [CrossRef]
30. Ullah, Z.; Zaman, G.; Ishak, A. Magnetohydrodynamic tangent hyperbolic fluid flow past a stretching sheet. *Chin. J. Phys.* **2020**, *66*, 258–268. [CrossRef]
31. Platt, J.R. Bioconvection zatterns in cultures of free-swimming organisms. *Science* **1961**, *133*, 1766–1767. [CrossRef] [PubMed]
32. Ferdows, M.; Zaimi, K.; Rashad, A.M.; Nabwey, H.A. MHD bioconvection flow and heat transfer of nanofluid through an exponentially stretchable sheet. *Symmetry* **2020**, *12*, 692. [CrossRef]
33. Alsenafi, A.; Bég, O.A.; Ferdows, M.; Bég, T.A.; Kadir, A. Numerical study of nano-biofilm stagnation flow from a nonlinear stretching/shrinking surface with variable nanofluid and bioconvection transport properties. *Sci. Rep.* **2021**, *11*, 1–21.
34. Waqas, H.; Khan, S.U.; Hassan, M.; Bhatti, M.M.; Imran, M. Analysis on the bioconvection flow of modified second-grade nanofluid containing gyrotactic microorganisms and nanoparticles. *J. Mol. Liq.* **2019**, *291*, 111231. [CrossRef]
35. Ayodeji, F.; Tope, A.; Samuel, O. Magneto-hydrodynamics (MHD) bioconvection nanofluid slip flow over a stretching sheet with microorganism concentration and bioconvection Péclet number effects. *Am. J. Mech. Ind. Eng.* **2019**, *4*, 86–95. [CrossRef]
36. Pal, D.; Mondal, S.K. MHD nanofluid bioconvection over an exponentially stretching sheet in the presence of gyrotactic microorganisms and thermal radiation. *BioNanoScience* **2018**, *8*, 272–287. [CrossRef]
37. Alshomrani, A.S. Numerical investigation for bio-convection flow of viscoelastic nanofluid with magnetic dipole and motile microorganisms. *Arab. J. Sci. Eng.* **2021**, *46*, 5945–5956. [CrossRef]
38. Zhao, M.; Xiao, Y.; Wang, S. Linear stability of thermal-bioconvection in a suspension of gyrotactic micro-organisms. *Int. J. Heat Mass Transf.* **2018**, *126*, 95–102. [CrossRef]
39. Zadeh, S.M.H.; Mehryan, S.A.M.; Sheremet, M.A.; Izadi, M.; Ghodrat, M. Numerical study of mixed bio-convection associated with a micropolar fluid. *Therm. Sci. Eng. Prog.* **2020**, *18*, 100539.
40. Jawad, M.; Shehzad, K.; Safdar, R.; Hussain, S. Novel computational study on MHD flow of nanofluid flow with gyrotactic microorganism due to porous stretching sheet. *Punjab Univ. J. Math.* **2020**, *52*, 43–60.
41. BAbd-el-Malek, M.; ABadran, N.; MAmin, A.; MHanafy, A. Lie Symmetry Group for Unsteady Free Convection Boundary-Layer Flow over a Vertical Surface. *Symmetry* **2021**, *13*, 175. [CrossRef]
42. Lund, L.A.; Omar, Z.; Dero, S.; Baleanu, D.; Khan, I. Rotating 3D flow of hybrid nanofluid on exponentially shrinking sheet: Symmetrical solution and duality. *Symmetry* **2020**, *12*, 1637. [CrossRef]
43. Sindhu, T.N.; Atangana, A. Reliability analysis incorporating exponentiated inverse Weibull distribution and inverse power law. *Qual. Reliab. Eng. Int.* **2021**, *37*, 2399–2422. [CrossRef]
44. Shafiq, A.; Hammouch, Z.; Sindhu, T.N. Bioconvective MHD flow of tangent hyperbolic nanofluid with newtonian heating. *Int. J. Mech. Sci.* **2017**, *133*, 759–766. [CrossRef]
45. Reddy, N.N.; Rao, V.S.; Reddy, B.R. Chemical reaction impact on MHD natural convection flow through porous medium past an exponentially stretching sheet in presence of heat source/sink and viscous dissipation. *Case Stud. Therm. Eng.* **2021**, *25*, 100879. [CrossRef]
46. Kameswaran, P.K.; Narayana, M.; Sibanda, P.; Makanda, G. On radiation effects on hydromagnetic Newtonian liquid flow due to an exponential stretching sheet. *Bound. Value Probl.* **2016**, *2012*, 1–16. [CrossRef]
47. Ishak, A. MHD boundary layer flow due to an exponentially stretching sheet with radiation effect. *Sains Malays.* **2011**, *40*, 391–395.
48. Alsaedi, A.; Khan, M.I.; Farooq, M.; Gull, N.; Hayat, T. Magnetohydrodynamic (MHD) stratified bioconvective flow of nanofluid due to gyrotactic microorganisms. *Adv. Powder Technol.* **2017**, *28*, 288–298. [CrossRef]
49. Shateyi, S.; Muzara, H. On the numerical analysis of unsteady MHD boundary layer flow of Williamson fluid Over a stretching sheet and heat and mass transfers. *Computation* **2020**, *8*, 55. [CrossRef]
50. Salahuddin, T.; Arshad, M.; Siddique, N.; Alqahtani, A.S.; Malik, M.Y. Thermophyical properties and internal energy change in Casson fluid flow along with activation energy. *Ain Shams Eng. J.* **2020**, *11*, 1355–1365. [CrossRef]
51. Mukhopadhyay, S. Slip effects on MHD boundary layer flow over an exponentially stretching sheet with suction/blowing and thermal radiation. *Ain Shams Eng. J.* **2013**, *4*, 485–491. [CrossRef]